Supplementary information to:

A low-cost low-maintenance ultraviolet lithography light source based on light-emitting diodes

Michael Erickstad[1], Edgar Gutierrez[1], and Alex Groisman[1,*]

The LED UV-light source was primarily designed for contact lithography of SU8 on silicon wafers to make master molds intended for casting microfluidic devices in PDMS. The main objectives were that the profiles of the PDMS microchannels be near-rectangular and that identical features on a photomask produce channels with identical profiles over the entire target area of 90×90 mm for a broad range of microchannel depths. Therefore, to test the performance of the LED light source, we used a photomask with a 5×5 array of 18 mm squares with identical test patterns, each having four clusters of arrays of transparent strips. Each cluster had five arrays with four strips each: 23 μm wide with 17 μm separations, 41 μm wide with 39 μm separations, 82 μm wide with 78 μm separations, 160 μm wide strips 80 μm separations, four 163 μm wide with 157 μm separations (Fig. 3a in the main text). The relatively broad range of the strip widths made it possible to obtain features of high aspect ratio with SU8 coatings with a broad range of thicknesses using a single photomask.

To examine the cross-sections of the microchannels, the PDMS casts were cut into 25 separate chips (18 mm squares), corresponding to the 5×5 array of test patterns on the photomask. Each 18 mm square chip was then cut into 4 small chips, one for each cluster of strips in each 18 mm square on the photomask (with a different exposure time for each small chip). To examine cross-sections of microchannels in a given small chip, the chip was carefully sliced with a razor blade in the direction across the microchannels (red rectangle in Fig. 3a), and the slice was photographed under a darkfield microscope. Each dark field micrograph was preprocessed using ImageJ software (NIH). First, a micrograph was rotated to ensure that the edge of the chip was horizontal. Second, a threshold was applied to convert the micrograph into a binary image, with the PDMS walls becoming white pixels and the rest becoming black pixels.

Next, the micrograph was processed using a homemade code in MATLAB (2012a, Mathworks, Natick, MA). The code displays a micrograph with channel cross-sections, allowing the user to select a rectangular region of interest (ROI) around a microchannel. The user selects the ROI such that the channel is completely contained in

[1] Department of Physics, University of California, San Diego, 9500 Gilman Drive, MC 0374, La Jolla, CA, 92093, USA
[*] Corresponding author, e-mail: agroisman@ucsd.edu

the rectangle, and the top and bottom of the channel match the top and bottom edges of the rectangle. The code then measures the width of the channel at each horizontal row of pixels within the ROI by counting the number of black pixels that the row contains. The code returns a list of widths vs. positions along the depth. The code also returns the depth of the channel calculated from the height of the ROI. The corners of the PDMS microchannels in the micrographs were slightly rounded both at the top (at chip surface) and the bottom. Therefore, to obtain reliable values for the channel width, it was necessary to exclude the data from several pixel rows at the top and bottom of each microchannel. For the 160 and 311 μm deep microchannels, 15 pixels (~9.6 μm) were excluded from the analysis on either end. For the 25 μm microchannels, 5 pixels (~1.6 μm) were excluded on either end.

The main source of variability between SU8 ridges produced by the exposure through transparent strips of the same width (and between cross-sections of microchannels, which were replicas of these ridges) was expected to be the variations of the UV illumination on length scales >25 mm. The length of 25 mm is one half of the distance between LEDs in the array. It is also the distance from the center of the light spot of a single LED, at which the intensity of light drops by ~20% (Fig. S-3). Whereas the 18 mm distance between the identical patterns on the photomask was comparable with this length, the distance between microchannels produced by identical transparent strips in an array of four on the photomask was much smaller (<1 mm). Therefore, the quality of the UV illumination was examined by choosing a single microchannel from each 18 mm square of the 5×5 array, carefully measuring cross-section of the microchannel, and comparing cross-sections of the 25 microchannels. The darkfield micrographs of the cross-channel slices of the PDMS chips (Fig. 3c in the main text and Fig. S-7-9) typically had multiple bright spots, corresponding to light scattering centers created by the cutting of PDMS. Therefore, the main factor in the selection of a single channel from an array of four (produced by near-even UV-illumination through identical transparent strips; Fig. 3b and Fig. S-7-9) was the smallest number of bright spots near the channel boundaries.

The cross-section of each channel was reduced to 5 numbers: channel depth, average width, SD of the width, and maximum and minimum of the width. These numbers are plotted in Fig. 4 in the main text and in Fig. S-8 and S-9. To quantify the variations of the average width between different channels, the minimal and the maximal average channel width amongst the 25 channels were found, and the mean and SD of the average widths of the 25 channels were calculated (Table S-1a, columns 4 – 7). To quantify the variability of profiles between different channels, the peak-to-peak and SD of variation of widths vs. depth of individual channels were compared, and the minimal,

maximal and average values of these parameters were calculated (Table S-1b, columns 1 – 6). Those numbers were then normalized to the average depth of respective channels (Table S-1b, columns 7 – 12).

As stated above, the UV-illumination had a high uniformity on small scales (<1 mm). Therefore, possible non-uniformity of the channel profiles within the arrays of four would be due to factors other than non-uniformity of illumination: imperfections in the SU8 resist, photomask, casting of PDMS, the cutting process, the darkfield micrography, and digital processing of the micrograph. To evaluate the contribution of these imperfections, we analyzed profiles of all channels in the clusters of four in Fig. 3b in the main text. (Those microchannels were cast from the 311 μm tall SU8 relief exposed for 6 min through 82 μm wide transparent strips with 78 μm separations in the representative regions 1, 2, 3, 7, 8, and 13 of the 5×5 test pattern; cf. Fig. 3b in the main text.) As before, the cross-section of each channel was reduced to 5 numbers: channel depth, average width, SD of the width, and maximum and minimum of the widths (Fig. S-6). The data indicated that, as expected, the variability between channels from the same array was smaller than the variability between channels in arrays from different test areas. However, the two levels of variability were comparable and were close to the resolution of our measurement technique (which was limited by the aforementioned technical factors).

a

depth, μm		channel width averaged over depth, μm				
mean	SD	mask	min	mean	max	SD
25	1.1	23	23	26	28	1.4
160	28	82	87	92	95	1.8
311	11	82	92	96	102	2.4

b

peak-to-peak variation of width, μm			SD of width, μm			peak-to-peak variation of width, %			CV of width, %		
min	mean	max	min	mean	max	min	mean	max	min	mean	max
1.9	3.4	8.0	0.4	0.7	1.1	7.7	13.6	32	1.4	2.9	4.5
2.6	5.8	12.8	0.7	1.4	3.1	1.6	3.7	8.0	0.4	0.9	1.9
4.5	8.1	14.0	1.2	2.2	4.3	1.4	2.6	4.5	0.4	0.7	1.4

Supplementary Table S-1. Various statistical parameters of microchannels in PDMS chips cast from silicon wafers spin-coated with 25, 160, and 311 μm thick layers of SU8 and exposed to UV-light from the LED source through the test photomask. The statistics are for channels cast from 25 regions of a wafer, corresponding to different copies of the test pattern in the 5×5 array on the photomask. The exposure times were 3, 4, and 6 min for 25, 160, and 311 μm thick layers of SU8, respectively. The values in the last six columns are normalized to the mean channel depths. Table b is a continuation of Table a.

Supplementary Figures:

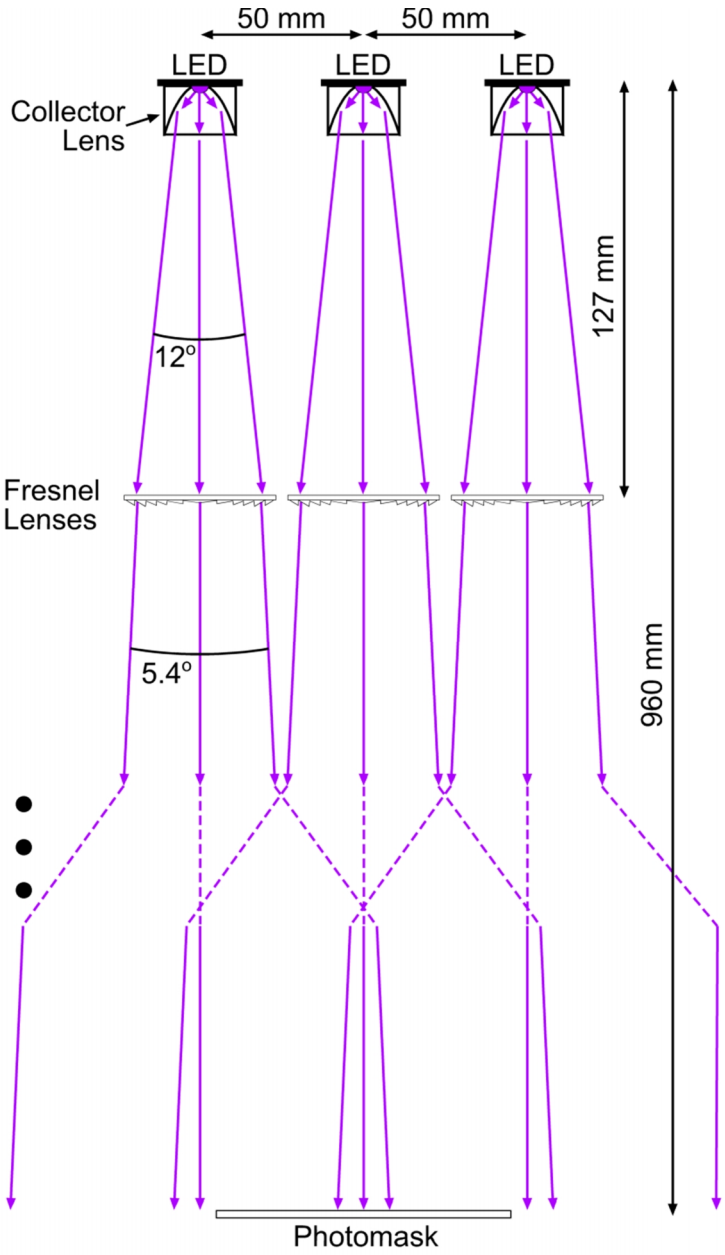

Figure S-1. Schematic of the optical setup of the LED UV-light source. A single row of the 3×3 LED array is shown. Three rays that are shown to emanate from each LED are the central ray, which corresponds to the maximum light intensity, and two rays at the angles where the light intensity is reduced to a half of the maximum. The region between the Fresnel lenses and the photomask is drawn with a break, which is labeled by three black dots, and parts of individual rays above and below the break are connected by dashed lines.

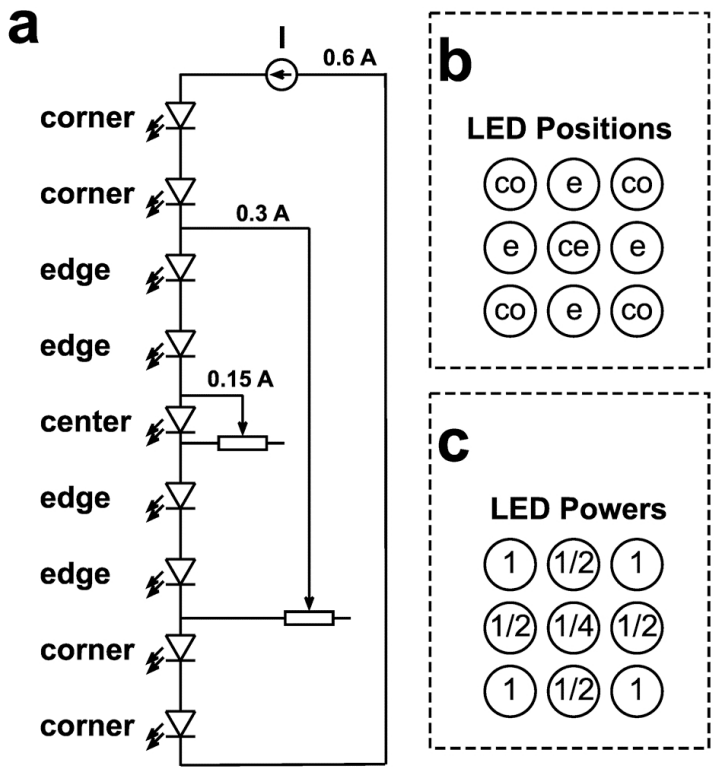

Figure S-2. LED intensity control scheme. (a) Circuit diagram with the current source, two potentiometers, and the 9 LEDs labeled as corner, edge, or center, according to their positions in the 3×3 array. (b) Schematic diagram defining the positions of the LEDs in the array, where “co” stands for corner, “ce” stands for center, and “e” stands for edge. (c) Schematic diagram showing the approximate relative luminous powers of the LEDs in the array, with the relative power of 1 corresponding to 0.6 A of current through the LED.

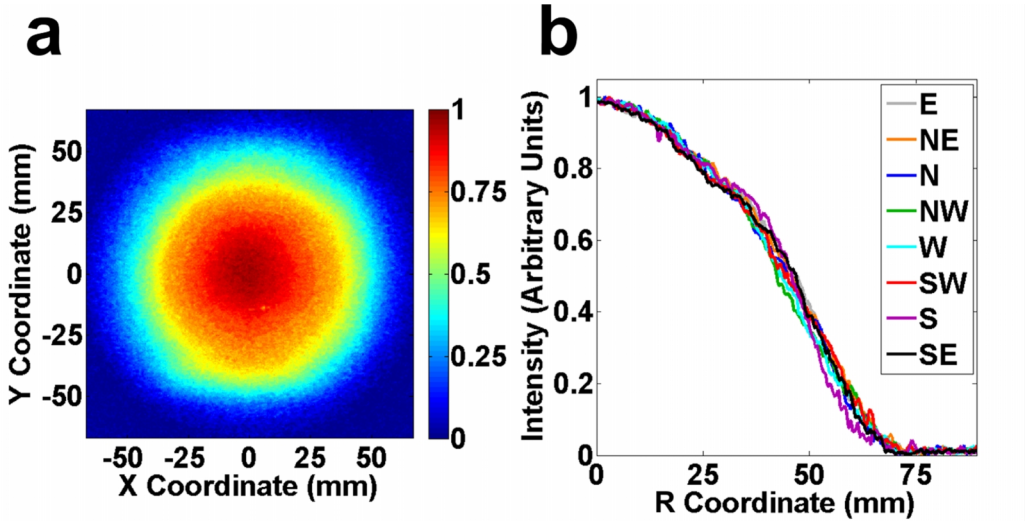

Figure S-3. The illumination field of a single LED in the array from a photograph. (a) A color-coded map of the light intensity from a photographic image of white paper illuminated by a single LED of the array. (b) Distribution of the illumination intensity in the photograph in panel **a** along lines extending radially from the center along 8 different directions, with E corresponding to the direction to the left (east), N – to the direction to the top (north), etc. Each plot is an average over a width of ~3.4 mm (16 pixels).

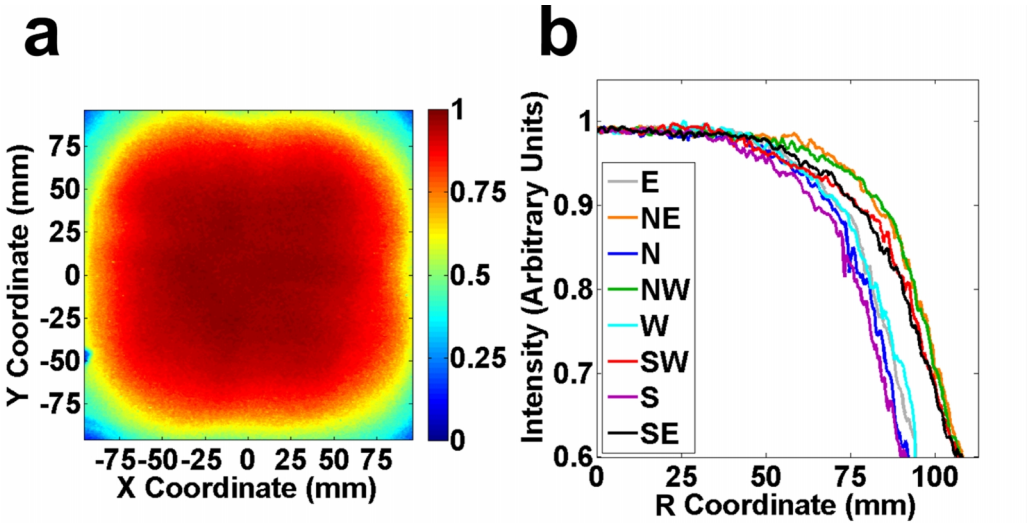

Figure S-4. The illumination field of the 3×3 LED array from a photograph. (a) A color-coded map of the light intensity from a photographic image of white paper illuminated by the LED array. (b) Distribution of the illumination intensity in the photograph in panel **a** along lines extending radially from the center along 8 different directions, with E corresponding to the direction to the left (east), N – to the direction to the top (north), etc. Each plot is an average over a width of 3.6 mm (16 pixels).

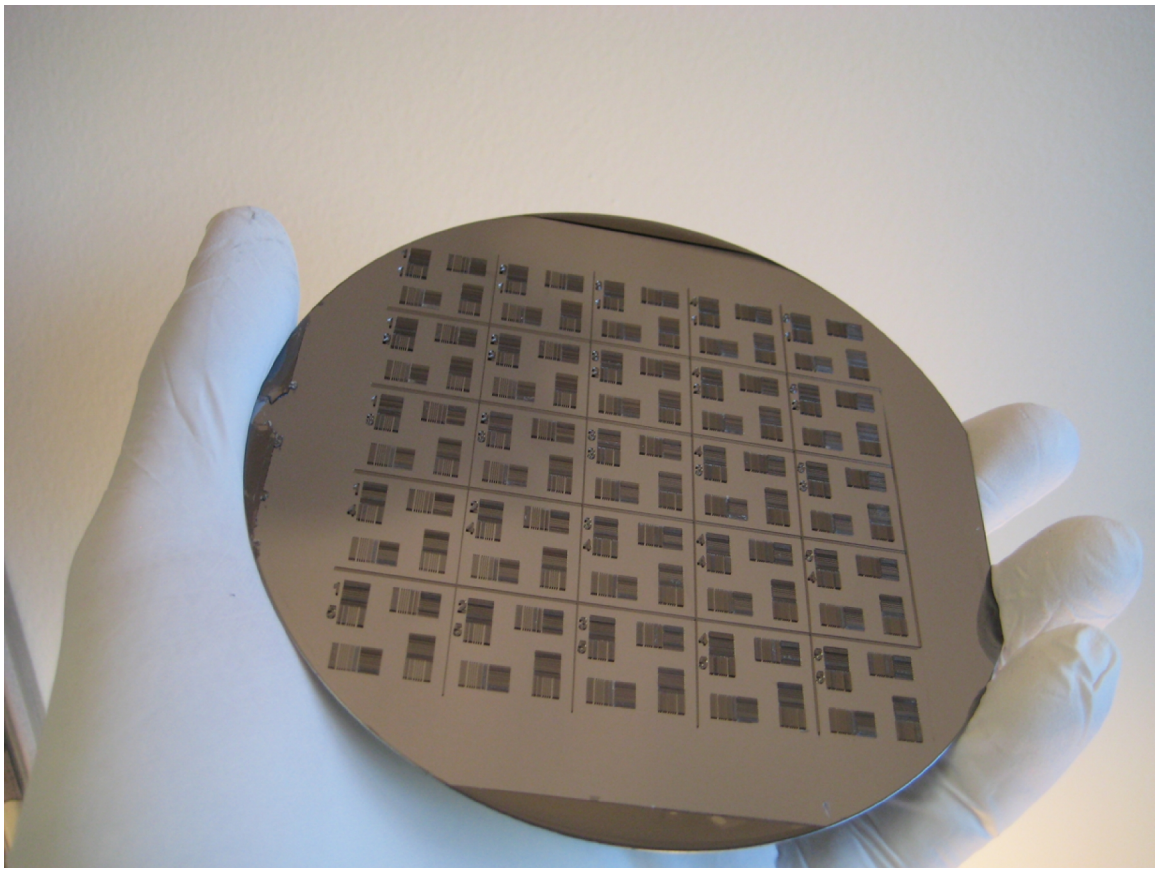

Figure S-5. A master mold obtained by the exposure of a 5 inch silicon wafer coated with a 311 µm layer of SU8 by UV-light from the LED light source through a photomask with a 5×5 array of identical test patterns. The patterns are numbered by their columns and rows. Each test pattern has 4 clusters of SU8 ridges. The clusters in the top left, bottom left, bottom right, and top right corners of each test pattern were produced by 4, 6, 8, and 10 min of UV exposure, respectively.

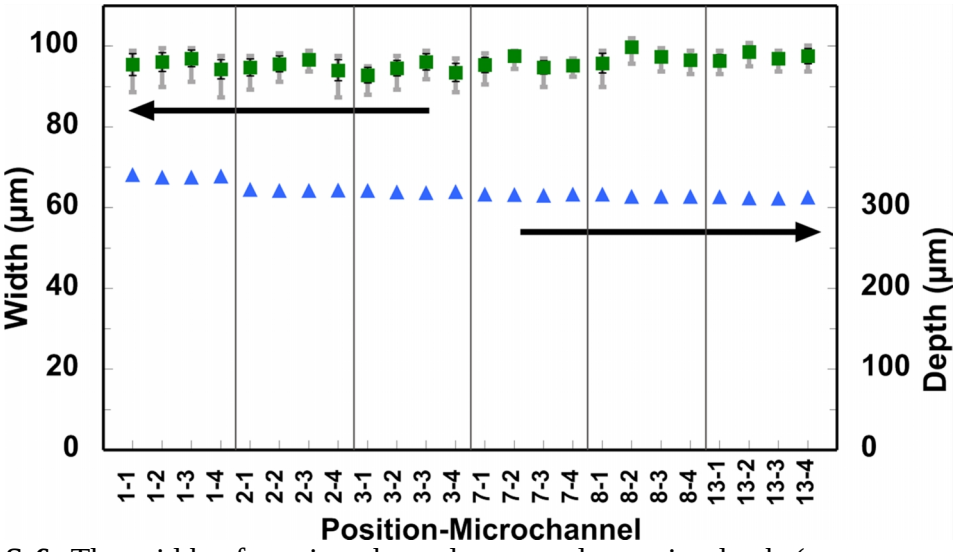

Figure S-6. The width of a microchannel averaged over its depth (green squares) and microchannel depth (blue triangles) for each of the 4 microchannels at 6 representative positions (cf. Fig. 3b in the main text) within the 5×5 test pattern array (positions 1, 2, 3, 7, 8, and 13). All microchannels are replicas of ridges produced by a 6 min UV exposure of a 311 µm thick (on average) layer of SU8 through 82 µm transparent strips with 82 µm separations. Black error bars show standard deviations of the widths; grey error bars show ranges of widths measured.

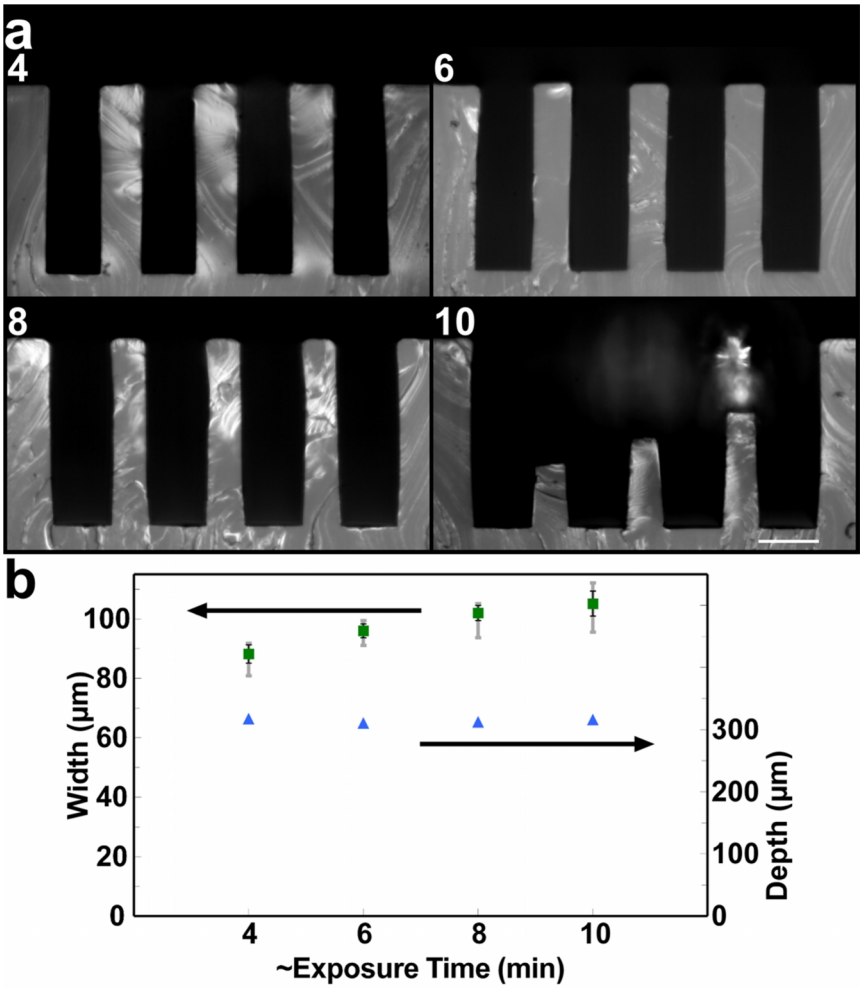

Figure S-7. Microchannels in PDMS chips that are replicas of SU8 ridges produced with different times of exposure of a 311 µm layer (average thickness) of SU8 to UV light from the LED source. (a) Micrographs of cross-sections of microchannels that are replicas of SU8 ridges produced with 4, 6, 8, and 10 min exposures to UV through 82 µm transparent strips with 78 µm separations in the central region of the wafer (#13 in Figure 3b in the main text). The micrographs are taken with a 10x objective under darkfield illumination. Scale bar 100 µm. (b) The microchannel width averaged over its depth (green squares) and the microchannel depth (blue triangles) for the microchannel cross-sections in panel **a**. (For the 10 min exposure only a 173 µm tall intact portion of the microchannel on the right was used for the measurements.) Black error bars show standard deviations of the widths; grey error bars show ranges of widths measured.

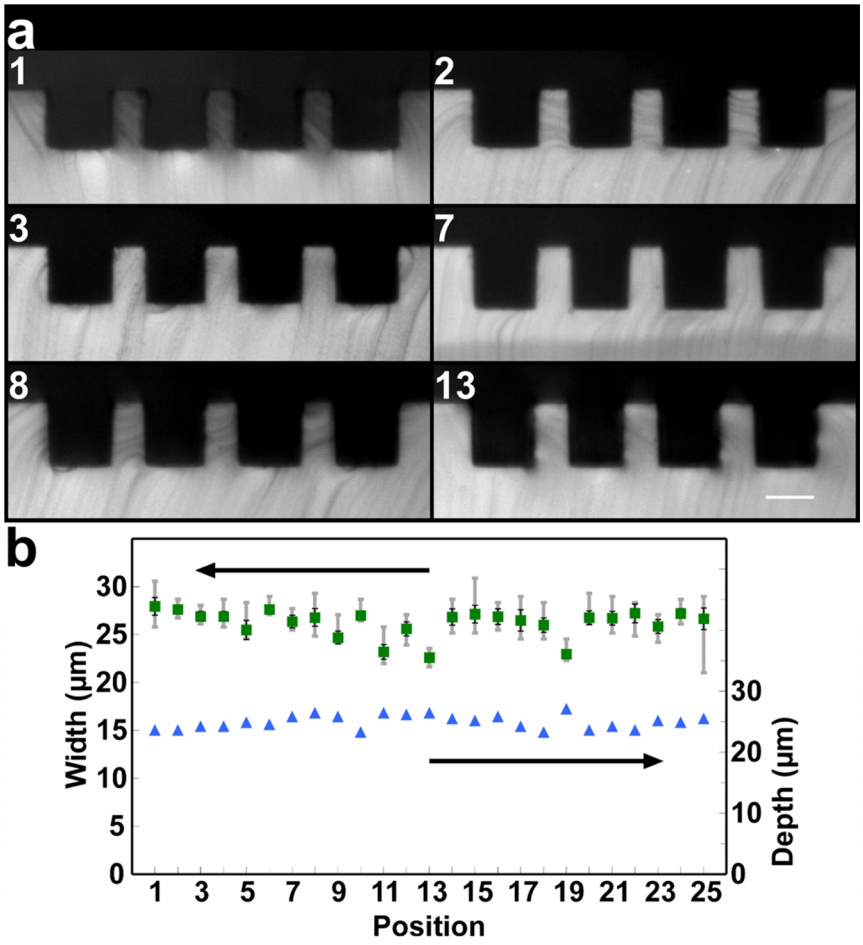

Figure S-8. PDMS chips with microchannels that are replicas of SU8 ridges produced by a 3 min exposure of a 25 µm layer of SU8 (average thickness) to UV-light through 23 µm wide transparent strips with 17 µm separations on the test photomask. (a) Micrographs of cross-sections of microchannels in PDMS chips cast from 6 representative regions of the wafer with different locations within the 5×5 test pattern array, as indicated by numbers, corresponding to the highlighted squares in Fig. 3b in the main text. The micrographs are taken with a 10x objective under darkfield illumination. Scale bar 25 µm. (b) The width of a microchannel averaged over its depth (green squares) and microchannel depth (blue triangles) for all 25 position within the 5×5 test pattern array (cf. Fig. 3b in the main text). Black error bars show standard deviations of the widths; grey error bars show ranges of widths measured.

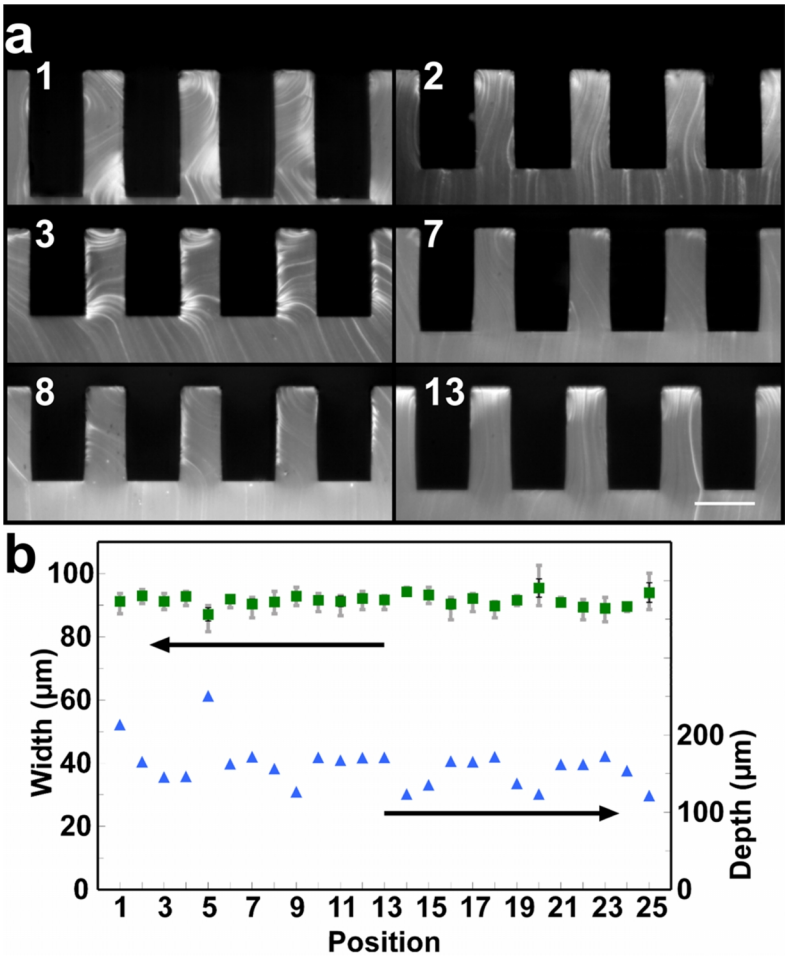

Figure S-9. PDMS chips with microchannels that are replicas of SU8 ridges produced by a 4 min exposure of a 160 µm layer of SU8 (average thickness) to UV-light through 82 µm wide transparent strips with 78 µm separations on the test photomask. (a) Micrographs of cross-sections of microchannels in PDMS chips cast from 6 representative regions of the wafer with different locations within the 5×5 test pattern array, as indicated by numbers, corresponding to the highlighted squares in Fig. 3b in the main text. The micrographs are taken with a 10x objective under darkfield illumination. Scale bar 100 µm. (b) The width of a microchannel averaged over its depth (green squares) and microchannel depth (blue triangles) for all 25 position within the 5×5 test pattern array (cf. Fig. 3b in the main text). Black error bars show standard deviations of the widths; grey error bars show ranges of widths measured.

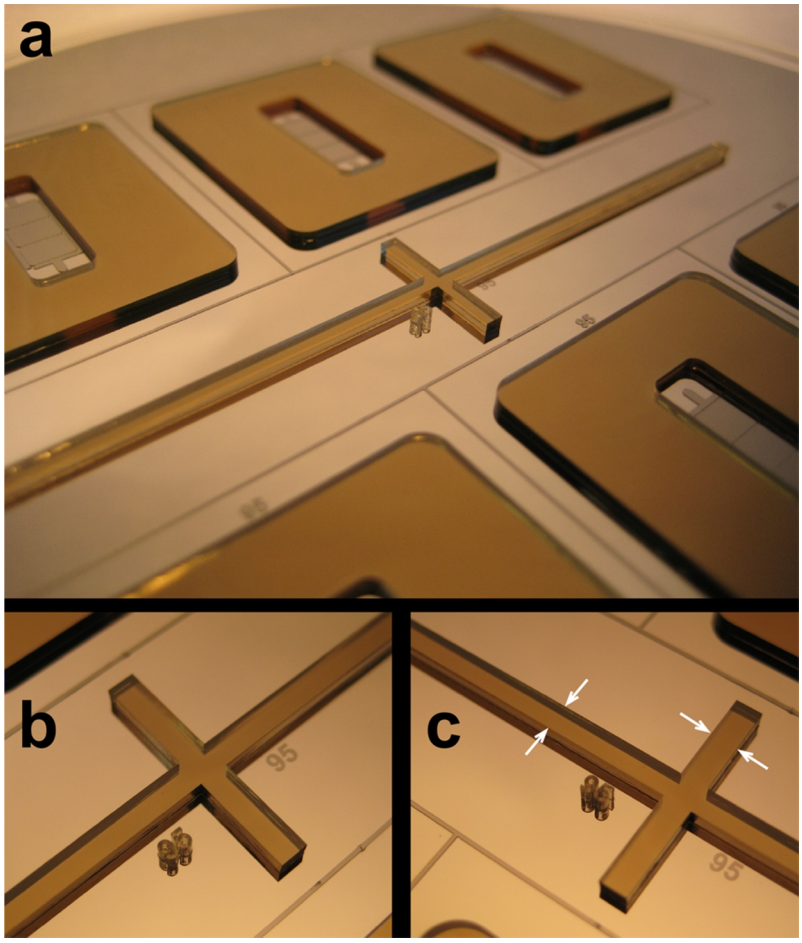

Figure S-10. Photographs of a wafer with ~1 mm tall SU8 relief produced using the LED UV-light source. The wafer also has ~40 µm tall SU8 features. Panels b and c are photographs of fragments of the relief in panel **a** taken from different angles with greater magnifications. Distances between the juxtaposed white arrows are 1.5 mm.

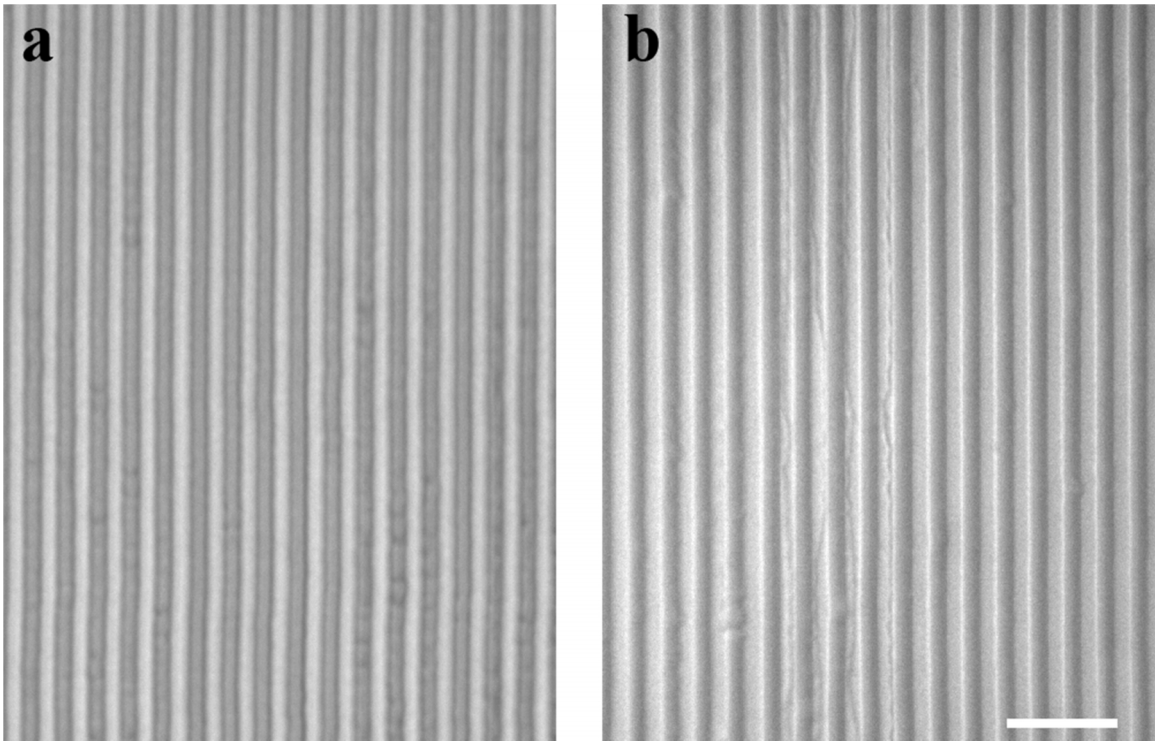

Figure S-11. Micrographs of a wafer with ~0.5 µm tall SU8 relief produced using the LED UV-light source and a high-resolution chrome mask. The chrome mask had periodic array of 1.5 µm wide transparent strips and 1.5 µm wide reflective strips between them. The exposure time was 10 min. The micrographs were taken under reflected brightfield illumination using an inspection microscope (Olympus BH) with (a) an Olympus Neo 40x/0.65 objective and (b) Zeiss 63x/1.4 Planapo oil objective (the two micrographs are taken in slightly different regions of the wafer). The micrograph in panel b has a better resolution because of the higher numerical aperture of the objective, but poorer contrast, because the objective is not ideally suited for the microscope. Scale bar is 10 µm. The micrographs show that the 1.5 µm features of the photomask are transferred onto the SU8 photoresist with a high fidelity.

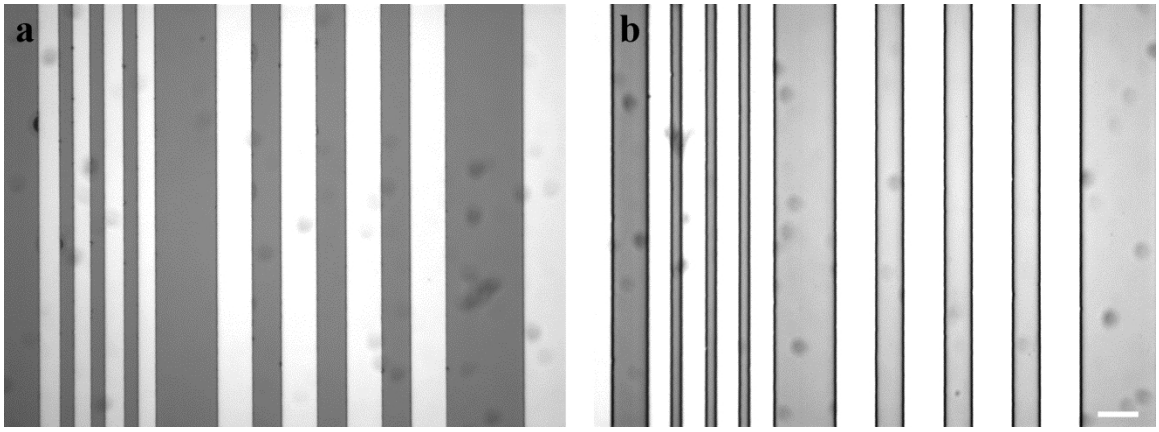

Figure S-12. Micrographs of wafers with reliefs of two different positive photoresists produced using the LED UV-light source. The photomask was the same as the one used to produce the 25, 160, and 311 μm tall reliefs of SU8 (Fig. 3 and Fig. S-5) and had a pattern of transparent and opaque strips of different widths. The micrographs were taken under reflected brightfield illumination using an inspection microscope (Olympus BH) with an Olympus Neo 5x/0.1 objective. Scale bar is 10 μm. (a) SPR 220-7.0 photoresist (by Dow Chemical Company). The photoresist was spin-coated at 2500 rpm for 30 sec; the wafer was baked on a hotplate with the temperature slowly ramped up from 65 to 115 °C and then let slowly cool down. The wafer was exposed to UV-light from the LED source for 10 min, post-exposure baked for 90 sec at 115 °C , and developed with Megaposit MF-26A developer (by Dow Electronic Materials). After development, the photoresist formed an ~8 μm relief with a pattern closely matching the pattern of transparent and opaque strips on the photomask. Specifically, one can see an array on the left, with four bright strips (wafer surface) and three dark strips between them (photoresist), which was produced by an array of four ~43 μm wide transparent strips and three ~37 μm wide opaque strips between them on the photomask. Another array of four bright strips and three dark strips in the middle of the micrograph was produced by an array of four ~82 μm wide transparent strips and three ~78 μm wide opaque strips between them on the photomask. (b) AZ40XT-11D photoresist (by AZ Electronic Materials). Coating, baking, and post-exposure baking followed the same protocol as for the SPR 220-7.0 photoresist, and the UV exposure time was also the same, at 10 min. The wafer was developed with the AZ300 developer (by AZ Electronic Materials). The micrograph shows a region of the wafer, which was exposed through nearly the same area of the photomask as the region of the wafer in panel a. The strips of the photoresist are ~7 μm narrower than the corresponding opaque strips on the photomask. (One can see that they are also somewhat narrower than the strips of the SPR 220 in panel a.) The reduced width of the strips of the photoresist likely resulted from a combination of the relatively large thickness of the photoresist, some overexposure, and the use of less than optimal development procedure. Nevertheless, there is an overall good matching between the pattern on the photomask and the pattern of the photoresist on the wafer.